Laboratory Investigation (2013) 93, 646–662

Lack of Cyp1b1 promotes the proliferative and migratory phenotype of perivascular supporting cells

Tammy L Palenski[1], Christine M Sorenson[2], Colin R Jefcoate[3] and Nader Sheibani[1,4]

Perivascular supporting cells, including pericytes and smooth muscle cells (PC/SMC), have an integral role during angiogenesis and control vascular remodeling, maturation, and stabilization of neoteric vessels. We recently showed that a Cyp1B1 deficiency in mice results in the attenuation of angiogenesis *in vivo* and the pro-angiogenic activity of endothelial cells *in vitro*. However, the contribution of PC/SMC, and more specifically the cell autonomous effects of Cyp1B1 in these processes, needs further investigation. Here we demonstrate that PC constitutively expressed Cyp1B1, and that a deficiency in Cyp1B1 was associated with enhanced proliferation, and decreased apoptosis. Mechanistically, the lack of Cyp1B1 was associated with increased oxidative stress and sustained NF-κB activation, which was reversed by the antioxidant *N*-acetylcysteine. These changes were also concomitant with alterations in PC migration, adhesion, and expression of various extracellular matrix proteins, including thrombospondin-2. Cyp1B1-deficient PC also expressed decreased levels of vascular endothelial growth factor. Together, our results suggest an important role for Cyp1B1 expression in the regulation of PC proliferation, migration, and survival through modulation of the intracellular oxidative state and NF-κB expression and/or activity. Thus, a lack of Cyp1B1 in PC may have a significant role in vascular dysfunction and integrity, contributing to the attenuation of angiogenesis.

Laboratory Investigation (2013) **93,** 646–662; doi:10.1038/labinvest.2013.55; published online 8 April 2013

KEYWORDS: angiogenesis; cell migration; extracellular matrix proteins; integrins; NF-KappaB; oxidative stress; signal transduction

Angiogenesis is a multistep process involving endothelial cell (EC) migration, proliferation and ultimately differentiation and formation of patent vessels. Endothelial cells stimulate the proliferation, migration, and recruitment of pericytes (PC) along the adjacent endothelial tubes by a steep gradient secretion of PDGF-BB from the tip cells.[1–3] PC embed in the basement membrane shared with EC and extend long cytoplasmic processes along the EC tubes on their abluminal surface, at times spanning several EC. Studies over the last two decades have begun to reveal the pivotal role PC have in synthesis, remodeling and maintenance of the vascular basement membrane, local regulation of vascular tone, and promoting vascular stability.[4] Vascular stability is attained through endothelial–PC interactions and concomitant deposition and remodeling of their extracellular matrix. Abnormal PC function is associated with many diseases including diabetic retinopathy, neonatal intraventricular hemorrhage, cancer, and some neurodegenerative disorders. However, current knowledge is still lacking regarding many aspects of endothelial–PC heterotypic interactions and more specifically the role PC have in microvessel homeostasis and maintenance.

Cytochrome P450 enzymes utilize endogenous substrates, such as eicosapentaenoic acid, retinoic acid, linoleic acid, and arachidonic acid, to generate intracellular messengers, such as *cis*-epoxyeicosatrienoic acids, mid-chain *cis-trans*-conjugated dienols, or ω-terminal alcohols, with important roles in the modulation of vascular tone, blood flow, and angiogenesis.[5] The cytochrome P450 enzymes have been identified within the vascular wall, including Cyp1A1, Cyp1B1, Cyp2J2, and Cyp2B6.[6] Cytochrome P450 1B1 (Cyp1B1) is an unusual member of the cytochrome P450 family of proteins. Gene structure reveals only two introns with a highly extended 3.5-kb 3′-UTR, and a promoter that is rich in GC islands.

[1]Department of Ophthalmology and Visual Sciences, University of Wisconsin School of Medicine and Public Health, Madison, WI, USA; [2]Department of Pediatrics, University of Wisconsin School of Medicine and Public Health, Madison, WI, USA; [3]Department of Cell and Regenerative Biology, University of Wisconsin School of Medicine and Public Health, Madison, WI, USA and [4]Department of Pharmacology, University of Wisconsin School of Medicine and Public Health, Madison, WI, USA
Correspondence: Dr N Sheibani, PhD, Department of Ophthalmology and Visual sciences, University of Wisconsin, 600 Highland Avenue, K6/456 CSC, Madison, WI 53792-4673, USA.
E-mail: nsheibanikar@wisc.edu

Received 15 November 2012; revised 12 February 2013; accepted 6 March 2013

Nucleic acid and amino-acid sequence analysis revealed Cyp1B1 to have only ~40% homology with Cyp1A1.

Expression of Cyp1B1 is conserved in the early embryo across several species during the development of the neural crest, hindbrain and eyes.[7–11] Cyp1B1 is constitutively expressed in extrahepatic epithelia, particularly mesenchymal cells and in stromal cells, including fibroblasts and vascular cells.[7,12–21] Cyp1B1 participates in the oxidative metabolism of xenobiotics, particularly the bioactivation of polycyclic aromatic hydrocarbons. Cyp1B1 metabolizes substrates of endogenous origin including retinol metabolism to retinal, the hydroxylation of melatonin, dietary plant flavanoids, and the formation of genotoxic catechol estrogens.[21–23] Cyp1B1 has been implicated in autosomal recessive primary congenital glaucoma,[24,25] conceivably as a result of maldevelopment of the eye anterior chamber angle.[26] However, the molecular and cellular mechanisms by which Cyp1B1 expression influence the development and maintenance of ocular function remains unknown.

Recent studies conducted in our laboratory have established an important role for Cyp1B1 in the regulation of vascular EC and angiogenesis.[14,27] *In vivo,* retinas from *Cyp1b1*-deficient (*cyp1b1* $-/-$) mice exhibited reduced vascular density and failed to undergo neovascularization during oxygen-induced ischemic retinopathy (OIR). We also observed decreased endothelial nitric oxide synthase (eNOS) staining in retinal blood vessels of *cyp1b1* $-/-$ mice compared with *cyp1b1* $+/+$ mice, especially during OIR. We showed that Cyp1B1 is constitutively expressed in the retinal vasculature and vascular EC, and that a deficiency in Cyp1B1 *in vitro* resulted in decreased migration, attenuation of eNOS expression, and capillary morphogenesis of retinal EC. These defects were mainly attributed to increased intracellular oxidative stress, and were relieved by decreases in oxygen level (2%) or addition of antioxidant, *N*-acetylcysteine (NAC).[14] We showed modulation of eNOS expression and NO synthesis, and/or its bioavailability is an important target of Cyp1B1-mediated EC function.[27] In addition, microarray studies show dramatic upregulation of Cyp1B1 by arterial levels of shear stress in cultures of human EC.[20] These results suggest an important role for Cyp1B1 in vascular development and homeostasis. However, expression of Cyp1B1 in perivascular supporting cells, including PC, and its deficiency on PC function remains to be explored.

Much investigation into the interactions between EC and PC has revealed that these two vascular cell types are interdependent, and that primary defects in one cell type may have obligatory consequences on the other.[28,29] However, the expression and function of Cyp1B1 in PC that invest the microvessels requires further investigation. Using transgenic mice that carry an interferon-γ-inducible temperature-sensitive large T antigen, we isolated PC from *cyp1b1* $+/+$ and *cyp1b1* $-/-$ mice. Here we demonstrate that Cyp1B1 is constitutively expressed in PC, and its deficiency leads to increased oxidative stress, sustained NF-κB p65 activation, and altered production of the matricellular proteins including increased expression of thrombospondin-2 (TSP2). These cells also exhibited alterations in the rate of proliferation and apoptosis, migration, adhesion to various extracellular matrix proteins, as well as their receptor expression, and decreased expression of vascular endothelial growth factor (VEGF). Together, our results suggest that the expression of Cyp1B1 in retinal PC is essential for maintaining the physiological function and integrity of the vasculature.

MATERIALS AND METHODS

Experimental Animals

All experiments were carried out in accordance to the Association for Research in Vision and Ophthalmology Statement for the Use of Animals in Ophthalmic and Vision Research and were approved by the Institutional Animal Care and Use Committee of the University of Wisconsin School of Medicine and Public Health. Immortomice expressing a temperature-sensitive simian virus 40 large T antigen (Charles River Laboratories, Wilmington, MA) were backcrossed into C57BL/6j mice in our laboratory, and further crossed with *cyp1b1* $-/-$ mice, and generated in a C57BL/6j background. The immorto-*cyp1b1* $-/-$ mice were identified by PCR analysis of DNA isolated from tail biopsies. The PCR primer sequences were as follows: immorto forward: 5′-CCTCTGAGCTATTCCAGAAGTAGTG-3′, immorto reverse: 5′-TTAGAGCTTTAAATCTCTGTAGGTAG-3′; Neomyacin forward: 5′-TTGGGTGGAGAGGCTATTCGGCTATGA-3′, Neomycin reverse: 5′-GGCGCGAGCCCCTGATGCTC-3′; Cyp1B1 forward: 5′-CTGAGTTGGACCAGGTTGTGG-3′; Cyp1B1 reverse: 5′-CATGGATTCTAAACGACTAGG-3′.

Tissue Preparation and Culture of Retinal PC

PC were isolated from mouse retinas by collecting retinas from one litter (6–7 pups, 4 weeks old) using a dissecting microscope. Twelve to fourteen retinas were rinsed with serum-free Dulbecco's Modified Eagle Medium (DMEM; Invitrogen, Carlsbad, CA), pooled in a 60-mm dish, minced, and digested for 45 min with collagenase type II (1 mg/ml, Worthington, Lakewood, NJ) with 0.1% BSA in serum-free DMEM at 37 °C. Cells were rinsed in DMEM containing 10% fetal bovine serum (FBS) and centrifuged for 5 min at 400 *g*. The digested tissue was resuspended in 4 ml DMEM containing 10% FBS, 2 mM L-glutamine, 100 μg/ml streptomycin, 100 U/ml penicillin, and murine recombinant IFN-γ (R&D Systems, Minneapolis, MN) at 44 U/ml, and evenly divided into 4 wells of a 24-well tissue culture plate and maintained at 33 °C with 5% CO_2. Cells were progressively passed to larger plates, maintained and propagated in 60-mm tissue culture dishes. These cells express a temperature-sensitive large T antigen whose expression is induced in the presence of INF-γ allowing the cells to readily propagate when cultured at 33 °C. The culture of these cells at 37 °C in the absence of INF-γ for 48 h results in loss of large T antigen.

Flow Cytometry

Flow cytometry was used to assess the expression of PC markers and integrins in *cyp1b1*+/+ and *cyp1b1*−/− PC. Confluent cultured *cyp1b1*+/+ and *cyp1b1*−/− PC from 60-mm culture plates were rinsed with phosphate-buffered saline (PBS) containing 0.04% EDTA and incubated with 1.5 ml of cell dissociation solution (Tris-buffered saline [20 mM Tris-HCl and 150 mM NaCl; pH 7.6] TBS containing 2 mM EDTA and 0.05% BSA). Cells were rinsed from plates with DMEM containing 10% FBS, washed once with 5 ml of TBS and blocked in 0.5 ml of TBS with 1% goat serum for 20 min on ice. Cells were centrifuged 5 min at 400 *g*, medium aspirated, resuspended in 0.5 ml TBS with 1% BSA containing an appropriate dilution of primary antibody (as recommended by the supplier), and incubated on ice for 30 min. Cells were incubated with rabbit anti-NG2 (Millipore AB5320; Temecula, CA), rabbit anti-mouse α-smooth muscle actin (Sigma; St Louis, MO), rat anti-mouse PECAM-1, anti-mouse CD36, rat-anti-mouse CD45, rat-anti-mouse Sca1, rat anti-mouse vascular cell adhesion molecule-1 (VCAM-1) (BD Pharmingen, San Diego, CA), rat anti-mouse PDGFR-β, rat anti-mouse CD11b (eBioscience, San Diego, CA), rat anti-mouse CD47 (a gift of Dr. William A. Frazier, Washington University, St. Louis, MO), rat anti-mouse VEGF-R1, and rat anti-mouse VEGF-R2 (R&D Systems). For integrin expression analysis, rabbit anti-β1-integrin (Santa Cruz Biotechnology, Santa Cruz, CA), rabbit anti-β8-integrin, rabbit anti-α2-integrin, rabbit anti-α3-integrin, rabbit anti-α4-integrin, rat anti-α5-integrin, rabbit anti-α7-integrin, rabbit anti-αv-integrin, mouse anti-α5β1-integrin and mouse anti-αvβ3-integrin (Millipore) for 30 min on ice. Cells were washed twice with TBS with 1% BSA and incubated with the appropriate FITC-conjugated secondary antibody for 30 min on ice. Cells were then washed twice with TBS with 1% BSA, resuspended in 0.5 ml TBS with 1% BSA, and analyzed using the FACScan Caliber flow cytometer (Becton-Dickinson, San Jose, CA). The isotype control was FITC-labeled isotype IgG as specifically stated above. Ten thousand cells were analyzed for each sample and three independent experiments were performed with two different isolations of PC.

Cell Proliferation

Cell proliferation was performed by plating *cyp1b1*+/+ and *cyp1b1*−/− retinal PC at 1×10^4 in triplicate per time point in 60-mm tissue culture dishes. Cell numbers were counted every other day in triplicate for 7 days and fed on days they were not counted. The rate of DNA synthesis was measured using Click-iT EdU Alexa Fluor 488 kit as recommended by the supplier (Invitrogen). The assay measures incorporation of 5-ethynyl-2′-deoxyuridine (EdU), a nucleoside analogue of thymidine, during cell proliferation. *Cyp1b1*+/+ and *cyp1b1*−/− retinal PC were plated at 5×10^5 cells on 60-mm tissue culture dishes and were incubated with 10 μM EdU in PC medium for 2 h at 33 °C. DNA synthesis was analyzed by measuring incorporated EdU using the FACScan Caliber flow cytometer (Becton-Dickinson). Ten thousand cells were analyzed for each sample and three independent experiments were performed with two different isolation of PC.

Real-Time PCR Analysis

Cyp1b1+/+ and *cyp1b1*−/− PC were allowed to reach 90% confluence, rinsed twice with PBS, scraped from 60-mm tissue culture plates and transferred to Eppendorf tubes. Cells were centrifuged, immediately frozen in liquid nitrogen and stored at −80 °C until analysis. Total RNA was extracted by mirVana PARIS kit (Ambion) according to the manufacturer's instructions. The cDNA synthesis was performed using 1 μg of total RNA and Sprint RT Complete-Double PrePrimed kit from (Clontech, Mountain View, CA). A volume of 1 μl of each cDNA (dilution 1:10) was used as template in qPCR assays, performed in triplicate of three biological replicates on Mastercycler Realplex (Eppendorf, Hauppauge, NY) using the SYBR qPCR Premix (Clontech). Amplification parameters were as follows: 95 °C for 2 min; 40 cycles of amplification (95 °C for 15 s, 60 °C for 40 s); dissociation curve step (95 °C for 15 s, 60 °C for 15 s, 95 °C for 15 s). Standard curves were generated from known quantities for each target gene of linearized plasmid DNA. Ten times dilution series were used for each known target, which were amplified using SYBR-Green qPCR. The linear regression line for ng of DNA was determined from relative fluorescent units (RFU) at a threshold fluorescence value (Ct) to quantify gene targets from cell extracts by comparing the RFU at the Ct to the standard curve, normalized by the simultaneous amplification of Rpl13A, which was used as a housekeeping gene to normalize all samples. The PCR primer sequences were: Bax forward: 5′-CCAAGAAGCTGAGCGAGTGTCT-3′, reverse: 5′-AGCTCCATATTGCTGTCCAGTTC-3′; Bim-EL forward: 5′-AGTGTGACAGAGAAGGTGGACAATT-3′, reverse: 5′-GGG ATTACCTTGCGGTTCTGT-3′; Bcl-2 forward: 5′-GGAGA GCGTCAACAGGGAGA-3′, reverse: 5′-CAGCCAGGAGAAA TCAAACAGAG; TNF-α forward: 5′-ACCGTCAGCCGATTTG CTAT-3′, reverse: 5′-TTGACGGCAGAGAGG AGGTT-3′; MCP-1 forward: 5′-GTCTGTGCTGACCCCAAGAAG-3′, and reverse: 5′-TGGTTCCGATCCAGGTTTTTA-3′.

Apoptosis and Cell Viability

Apoptosis was determined by measuring caspase activation using Caspase-Glo 3/7-assay kit as recommended by the supplier (Promega, Madison, WI). The assay provides caspase-3/7 DEVD-aminoluciferin substrate and the caspase-3/7 activity is detected by luminescent signal. For the assay, *cyp1b1*+/+ and *cyp1b1*−/− PC were plated at 8×10^3 per well of a 96-well plate. As an oxidative or apoptotic stimulus, PC were incubated with 150 μM hydrogen peroxide (H_2O_2; Fisher Scientific, Fair Lawn, NJ) or 10 nM staurosporine (Invitrogen), in PC medium for 24 h at 33 °C. Caspase activity was detected using a luminescent microplate reader (Victa2 1420 Multilabel Counter, PerkinElmer; Waltham,

MA). All samples were prepared in triplicate and repeated at least three times with similar results. Cellular viability of PC was determined using the CellTiter 96 Aqueous Non-Radioactive cell proliferation assay (MTS; 3-(4,5-dimethylthiazol-2-yl)-5-(3-carboxymethoxyphenyl)-2-(4-sulfophenyl)-2H-tetrazolium; Promega). *Cyp1b1*+/+ and *cyp1b1*−/− PC were plated at 4×10^3 per well of a 96-well plate and incubated with 250 μM H_2O_2 for 48 h at 33 °C, and incubated further with MTS solution for 3 h. The viability was determined by measuring absorbance at 490 nm using a microplate reader (Thermomax, Molecular Devices, Sunnyvale, CA), and determined as a percentage of control untreated cells. All samples were prepared in triplicate and repeated at least three times with similar results.

Determination of the Level of Reactive Oxygen Species (ROS)

The levels of oxidative stress were determined by staining cells with dihydroethidium (DHE; Invitrogen). DHE is oxidized to red fluorescent ethidium by O_2—in the cytosol and interchalates in the DNA. Cells were plated at 5×10^4 cells in chamber slides (Lab-TEK; NUNC, Rochester, NY) coated with 2 μg/ml fibronectin (BD Biosciences, San Jose, CA) and incubated with 5 μM TMS (Cayman Chemical), 200 μM H_2O_2, 1 mM NAC or dimethyl sulfoxide (DMSO) for 24 h. Cells were loaded with 10 μM DHE for 20 min at 33 °C, washed with PC medium and returned to PC medium twice for two 30-min recovery periods. Fluorescent intensity was analyzed with a fluorescent microscope (Carl Zeiss Optical, Germany), and images were captured in digital format. Three independent experiments were performed. For quantitative assessment, the mean fluorescent intensities were determined using Image J 1.46a and representative images are shown.

Indirect Immunofluorescence

Cells were plated at 1×10^5 in chamber slides (Lab-TEK, NUNC) coated with 2 μg/ml fibronectin (BD Biosciences), washed in PBS, fixed with methanol for 15 min on ice, and blocked with 1% ovalbumin in TBS at 37 °C for 20 min. Slides were washed with TBS and incubated with anti-NG2 (1:200 dilution, Millipore) and anti-αSMA-FITC-conjugated (1:200 dilution, Sigma) in TBS containing 1% ovalbumin at 37 °C for 40 min. After washing with TBS, cells were incubated with appropriate Cy3-conjugated secondary antibody (1:500 dilution in TBS containing 1% ovalbumin) at 37 °C for 40 min. Cells were washed with TBS three times, mounted with a 1:1 TBS:glycerol solution with DAPI, and analyzed with a fluorescent microscope (Carl Zeiss Optical, Germany). Images were captured in digital format. Three independent experiments were performed and representative images are shown.

Scratch Wound Assay

Cells were plated at 8×10^5 cells in 60-mm tissue culture dishes and allowed to reach confluence. Cell monolayers were wounded with a 1-ml micropipette tip, rinsed with DMEM containing 10% FBS twice and fed with PC medium containing 1 μM 5-fluorouracil (Sigma) to exclude the potential contribution of cell proliferation to wound closure. The wound closure was monitored and photographed at 0, 24, 48 and 72 h using a phase microscope in digital format. For quantitative assessment, the distances migrated as percent of total distance were determined. All samples were repeated at least three times with two different isolations of PC with similar results.

Transwell Migration

Transwell filters (Corning, Acton, MA) were coated with 2 μg/ml fibronectin in PBS and incubated overnight at 4 °C. The bottom of the transwell was rinsed with PBS and blocked with 2% BSA in PBS for 1 h at room temperature. The transwell was rinsed with PBS, and 500 μl serum-free DMEM was added to the bottom of each well and 1×10^5 cells in 100 μl of serum-free medium were added to the top of the transwell membrane. Following 4 h in a 33 °C tissue culture incubator, the cells and medium were aspirated and the upper side of the membrane wiped with a cotton swab. The cells that had migrated through the membrane were fixed with 4% paraformaldehyde, stained with hematoxylin-eosin, and mounted on a slide. Ten high-power fields ($\times 200$) of cells were counted for each condition and the average and s.e.m. were determined. All samples were prepared in duplicate and the experiment repeated at least three times with similar results.

Cell Adhesion

Cell adhesion to various extracellular matrix proteins was performed as previously described.[30] Varying concentrations of fibronectin, human type I collagen, vitronectin, and laminin (BD Biosciences) prepared in TBS with $Ca^{2+}Mg^{2+}$ (2 mM each; TBS with $Ca^{2+}Mg^{2+}$) were coated on 96-well plates (50 μl per well; Nunc Maxisorbe plates, Fisher Scientific) overnight at 4 °C. Plates were then rinsed four times with TBS with $Ca^{2+}Mg^{2+}$ and blocked with 200 μl of 1% BSA prepared in TBS with $Ca^{2+}Mg^{2+}$ for at least 1 h at room temperature. Cells were removed using 1.5 ml of dissociation solution, washed once with TBS and resuspended at 5×10^5 cells per ml in HEPES-buffered saline (25 mM HEPES, pH 7.60, and 150 mM NaCl, 4 mg/ml BSA). After blocking, plates were rinsed with TBS $Ca^{2+}Mg^{2+}$ once, 50 μl of cell suspension was added to each well containing 50 μl of TBS with $Ca^{2+}Mg^{2+}$, and the cells were allowed to adhere for 90 min at 37 °C in a humidified incubator. Non-adherent cells were removed by gently washing the plate four times with 200 μl of TBS with $Ca^{2+}Mg^{2+}$ until no cells were left in wells coated with BSA. The number of adherent cells in each well was quantified by measuring the levels of intracellular acid phosphatase by lysing adherent cells in 100 μl of lysis buffer (50 mM sodium acetate pH 5.0, 1% Triton X-100, 4 mg/ml *p*-nitrophenyl

phosphate) and incubating at 4 °C overnight. The reaction was neutralized by adding 50 μl of 1 M NaOH and the absorbance was determined at 405 nm using a microplate reader (Thermomax, Molecular Devices). All samples were prepared in triplicate and experiments repeated at least three times with similar results.

Western Blot Analysis

Cells were plated at 5×10^5 in 60-mm culture dishes and allowed to reach ~90% confluence in 2 days. Cells were then rinsed once with serum-free DMEM and incubated with serum-free growth medium for 2 days. Conditioned medium was collected and clarified by centrifugation. Cells were rinsed once in 0.04% EDTA in PBS and lysed in 100 μl of lysis buffer (50 mM HEPES pH 7.5, 100 mM NaCl, 0.1 M EDTA, 1 mM $CaCl_2$, 1 mM $MgCl_2$, 1% Triton X-100, 1% NP-40, 0.5% deoxycholate, and protease inhibitor cocktail (Roche Biochemicals, Mannheim, Germany)), briefly sonicated and centrifuged at 14 000 *g* for 10 min at 4 °C. In some cases, total protein lysates were prepared from these samples in a modified lysis buffer (2 mM orthovandate, 2 mM sodium fluoride). Protein concentrations were determined using the bicinchoninic acid method (Pierce, Rockford, IL). Samples were adjusted for protein content (50 μg), mixed with appropriate volume of 6 × SDS-sample buffer, and analyzed by SDS-PAGE (4–20% Tris-glycine gels, Invitrogen). Proteins were transferred to nitrocellulose membrane and incubated in blocking buffer (0.05% Tween-20 and 5% skim milk in TBS) for 1 h at room temperature. Membranes were then incubated with mouse anti-human TSP1 (A6.1 Neo Markers, Fremont, CA), mouse anti-TSP2 (BD Pharmingen), rabbit anti-rat fibronectin, anti-β-actin (Sigma), rat anti-chicken tenascin-C (Milipore, AB19013), goat anti-mouse osteopontin, anti-VEGF-R1, anti-JNK, anti-phospho-JNK (R&D Systems), rabbit anti-Akt, rabbit anti-phospho-Akt, rabbit anti-Erk1/2, mouse anti-phospho-Erk1/2, rabbit anti-p38, rabbit anti-phospho-p38 (Cell Signaling), rabbit anti-p65, rabbit anti-phospho-p65, rabbit anti-STAT3, and mouse anti-phospho-STAT3 (Santa Cruz). Membranes were washed, incubated with horseradish-peroxidase-conjugated secondary antibody (1:5000, Jackson ImmunoResearch Laboratories, West Grove, PA) for 1 h at room temperature, and the protein was visualized according to the chemiluminescent procedure (Chemiluminescence reagent; GE Biosciences). The mean band intensities were measured densitometrically using Image J 1.46a.

Capillary Morphogenesis

Tissue culture plates (35 mm) were coated with 0.5 ml Matrigel (10 mg/ml; BD Bioscience) and allowed to harden at 37 °C for at least 30 min. Cells were removed using trypsin/EDTA, washed with DMEM containing 10% FBS, centrifuged at 400 *g* for 5 min, and suspended at 2×10^5 cells/ml in EC growth medium without serum. Retinal EC and PC were used at a 1:1 ratio. Cells in a 2-ml volume were applied to the Matrigel-coated plates and photographed after 18 h using a Nikon microscope in a digital format. For quantitative assessment of the data, the mean number of branch points was determined by counting the number of branch points in five fields (× 20). These experiments were repeated with three different isolation of cells.

VEGF Analysis

VEGF protein levels produced by *cyp1b1*+/+ and *cyp1b1*−/− PC were determined using a Mouse VEGF Immunoassay kit (R&D Systems). Cells were plated at 6×10^5 cells on 60-mm tissue culture dishes and allowed to reach ~90% confluence. The cells were then rinsed once with serum-free DMEM and were grown in serum-free medium for 2 days. Conditioned medium was centrifuged at 400 *g* for 5 min to remove cell debris, and 50 μl was used in the VEGF Immunoassay. The assay was performed in triplicate as recommended by the manufacturer and was normalized to the number of cells. The amount of VEGF was determined using a standard curve generated with known amounts of VEGF in the same experiment. These experiments were repeated three times with two different isolations of cells.

Statistical Analysis

Statistical differences between samples were evaluated when appropriate with student's unpaired *t*-test (two-tailed), two-way ANOVA with Bonferroni correction for multiple comparisons, or linear regression statistics to compare slopes for statistical significance. Data are represented as mean ± s.e.m. Each result is representative of at least three independent experiments. All statistical assessments were evaluated at the 0.05 level of significance. Statistical analyses were performed with GraphPad Prism statistical software (GraphPad Software, La Jolla, CA).

RESULTS

Cyp1B1 is Constitutively Expressed in Retinal PC

To gain insight into the cell autonomous role Cyp1B1 has in PC function, retinal PC were isolated from *cyp1b1*+/+ and *cyp1b1*−/− Immortomice. Both *cyp1b1*+/+ and *cyp1b1*−/− PC exhibited similar irregular, stellate morphology when plated on tissue culture plates (Figure 1a). We next assessed the expression of Cyp1B1 by western blot analysis of lysates prepared from *cyp1b1*+/+ and *cyp1b1*−/− retinal PC incubated with DMSO (control) or 2,3,7,8-Tetrachlorodibenzodioxin (TCDD; 10 nM) for 24 h. Figure 1b demonstrates constitutive expression Cyp1B1 in retinal PC, which was further induced in the presence of TCDD, a known inducer of Cyp1B1.[19] Cyp1B1 was absent in the *cyp1b1*−/− retinal PC as expected. Purified human Cyp1B1 protein was used as a positive control. Cyp1B1 was also expressed in PC prepared from vascular beds of other mouse tissues, including heart and kidney (Figure 1c). Others have also reported expression of Cyp1B1 in both human and

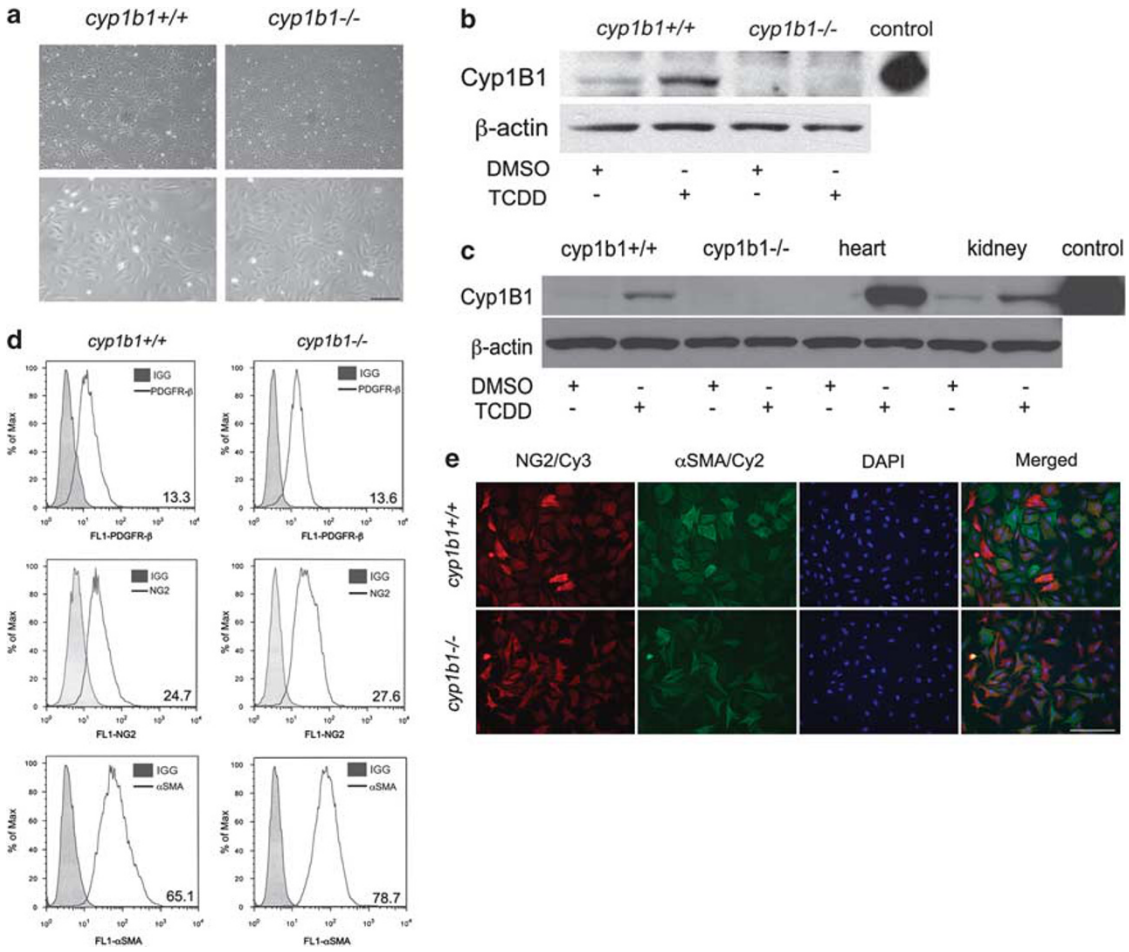

Figure 1 Isolation and characterization of mouse retinal pericytes (PC). (**a**) *Cyp1b1* +/+ and *cyp1b1* −/− PC were photographed in digital format at ×40 (top panels) and ×100 (bottom panels) magnification. Scale bar in top panel indicates 100 μm; bottom panels, 20 μm. (**b**,**c**) Cyp1B1 expression in retina, heart, and kidney PC incubated with dimethyl sulfoxide (DMSO) or 10 nM 2,3,7,8-Tetrachlorodibenzodioxin (TCDD) for 48 h was evaluated by western blot analysis of cell lysates (50 μg). Purified recombinant human Cyp1B1 protein was used as a positive control. β-actin was used to assess loading. (**d**) *Cyp1b1* +/+ and *cyp1b1* −/− PC were examined for expression of platelet-derived growth factor-β (PDGFR-β), neuroglia proteoglycan 2 (NG2), and alpha-smooth muscle actin (α-SMA) by flow cytometry. Representative mean fluorescent intensities are indicated in bottom right corner of each panel. (**e**) Indirect immunofluorescent staining using NG2 and αSMA was performed to demonstrate culture purity. DAPI was used to stain cell nuclei. Scale bars, 50 μm.

murine aortic vascular SMC, as well as PC in human colon tissues.[16,31,32] We next examined the PC marker expression to ensure these cells retained PC characteristics. *Cyp1b1* +/+ and *cyp1b1* −/− PC were positive for platelet-derived growth factor-receptor β (PDGF-Rβ), neuroglia proteoglycan 2 (NG2), and alpha-smooth muscle actin (αSMA) (Figure 1d). We also determined the purity of our retinal PC population via immunofluorescence staining using NG2, αSMA and DAPI (Figure 1e). Both cell types stained positive for NG2 and αSMA. Approximately 95% of the cells were positive for both NG2 and αSMA. Approximately 5% of the cells were only positive for NG2 or αSMA.

We analyzed the expression of other vascular cell markers in *cyp1b1* +/+ and *cyp1b1* −/− retinal PC by flow cytometry (Figure 2). As expected, PC did not express the endothelial-specific marker PECAM-1 or VEGF-R2, but expressed significant amounts of VEGF-R1, CD36 and VCAM-1. PC also expressed CD47, the thrombospondin-1 (TSP1) carboxyl terminal receptor, which is crucial for PC migration.[33] We also examined the presence of markers reported to be expressed by hematopoietic and mesenchymal stem cells, respectively, which are known for their potential to produce vascular supporting cells, including CD11b and Sca1.[34] We further assessed the levels of vascular endothelial growth factor-receptor 1 (VEGF-R1) by western blot analysis (Figure 2b). The quantitative assessment of the data revealed a 25% decrease in VEGF-R1 in the *cyp1b1* −/− PC compared with *cyp1b1* +/+ cells. *Cyp1b1* −/− PC exhibited an ~80% decrease in expression of VCAM-1 (Figure 2d) by flow cytometry.

Cyp1b1 −/− PC Exhibited Enhanced Proliferation

We next determined the impact of a *cyp1B1* deficiency on the rate of proliferation and apoptosis of PC. The rates of pro-

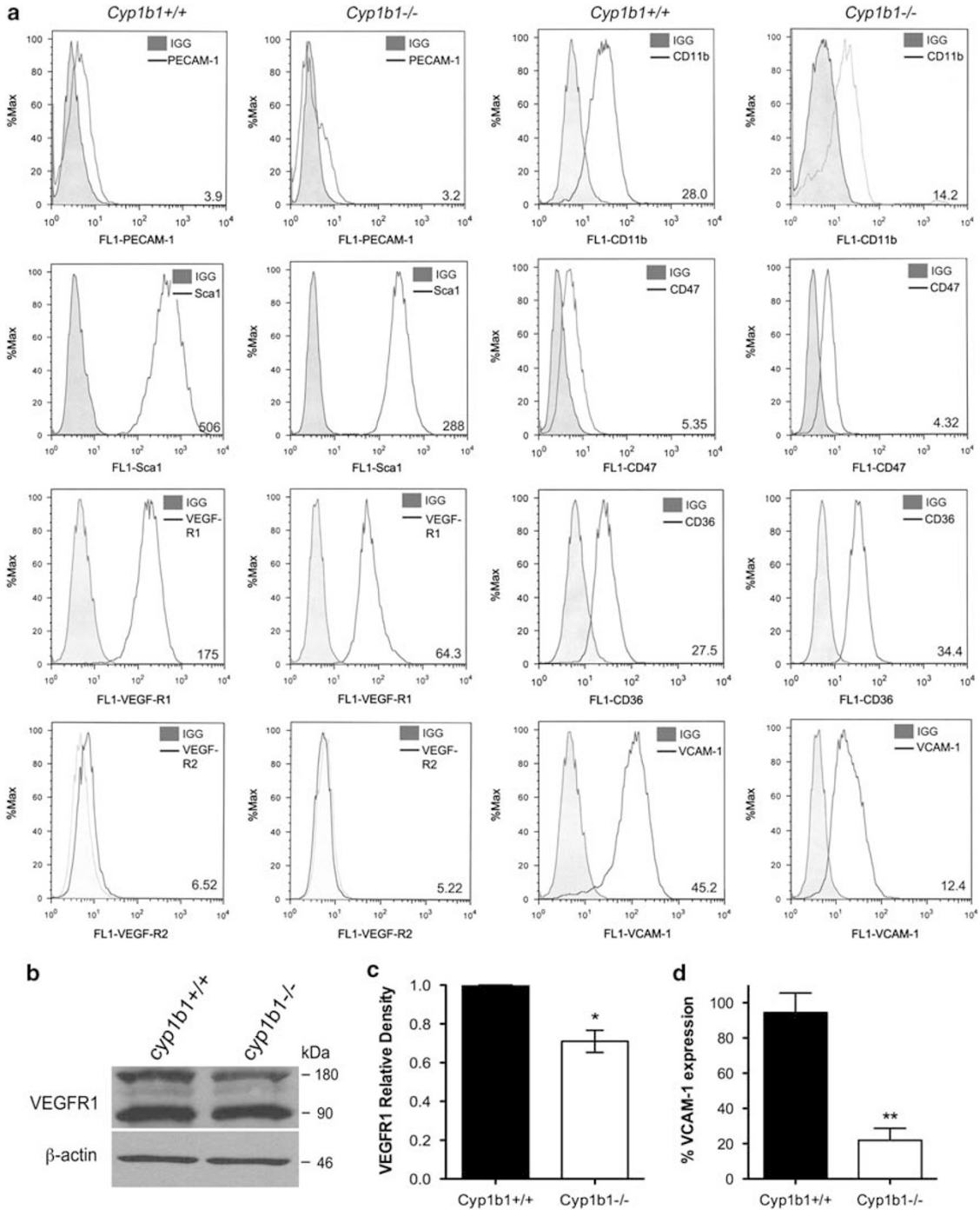

Figure 2 Retinal pericytes (PC) express other vascular cell markers. (**a**) Expression of PECAM-1, Sca1, VEGF-R1, VEGF-R2, CD11b, CD36, CD47, and VCAM-1 were determined by flow cytometry. Representative mean fluorescent intensities are indicated in bottom right corner of each panel. Shaded areas show staining in the absence of primary antibody. (**b**) Expression of VEGF-R1 was analyzed by western blot. A representative image is shown. (**c**) Mean relative density for VEGF-R1 was determined ($n=2$, $^{*}P<0.05$). (**d**) Percent expression of VCAM-1 was determined by flow cytometry ($N=3$, $^{**}P<0.01$).

liferation in *cyp1b1*+/+ and *cyp1b1*−/− PC were determined by counting the cell numbers. We observed a significant increase in proliferation of *cyp1b1*−/− PC compared with *cyp1b1*+/+ cells (Figure 3a). To determine whether the increased proliferation was due to an increased rate of DNA synthesis, we calculated the percentage of cells undergoing active DNA synthesis using EdU labeling. The *cyp1b1*−/− PC displayed comparable levels of DNA synthesis with *cyp1b1*+/+ PC (Figure 3b). We next addressed whether the increased proliferation was due to a decrease in the rate of apoptosis. Apoptotic cell death was determined by evaluation of the activation status of

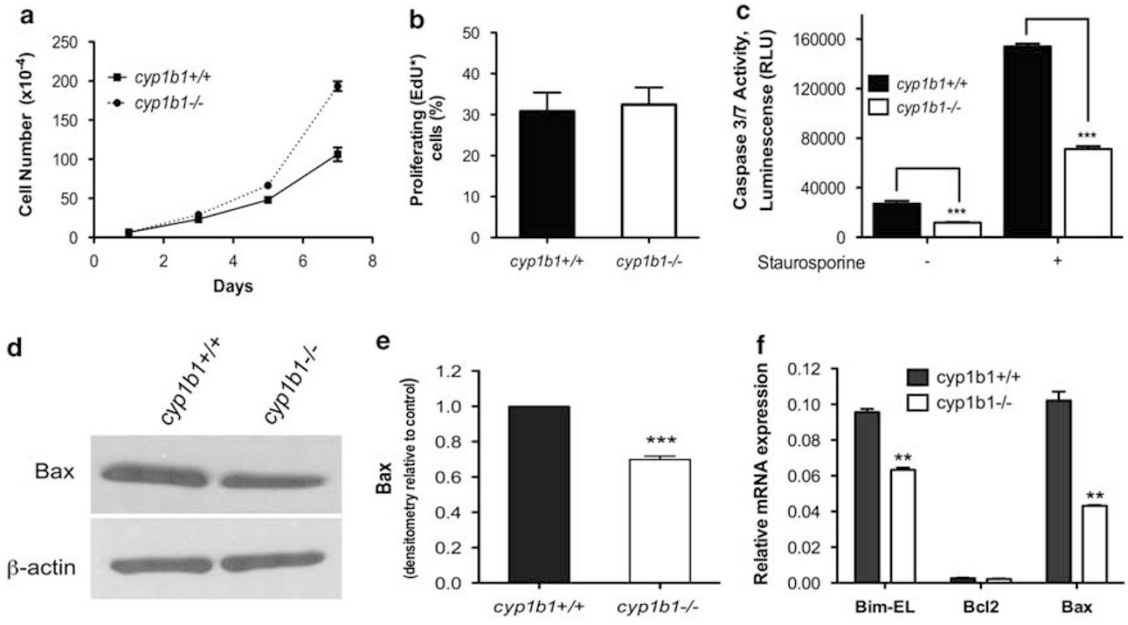

Figure 3 Lack of Cyp1B1 in retinal pericytes (PC) resulted in increased proliferation and decreased apoptosis. (**a**) The rate of cell proliferation was increased in *cyp1b1* −/− PC compared with wild-type cells by counting the cell numbers. (**b**) *Cyp1b1* +/+ and *cyp1b1* −/− PC display similar rates of DNA synthesis by flow cytometry ($P > 0.05$). (**c**) The rate of apoptosis was determined by measuring caspase activity with luminescent signal from caspase-3/7 DEVD-aminoluciferin substrate. *Cyp1b1* −/− PC demonstrated a twofold decrease in basal levels of caspase-3/7 and a twofold decrease when challenged with 10 nM staurosporine. RLU, relative luminescence unit. (**d**) Expression of Bax was analyzed by western blotting. The β-actin level was assessed as a loading control. (**e**) Quantification of band intensity demonstrated a 1.4-fold decrease in Bax expression in the *cyp1b1* −/− PC. (**$P < 0.001$, ***$P < 0.0001$). (**f**) Relative mRNA expression of Bim-EL, Bax, and Bcl-2 was analyzed by real-time PCR ($N = 3$, **$P < 0.001$).

caspase-3/7 in *cyp1b1* +/+ and *cyp1b1* −/− PC. The *cyp1b1* −/− PC displayed a twofold decrease in caspase-3/7 activation under basal conditions (Figure 3c). Staurosporine is a known inducer of apoptosis in many cell types. Upon challenge with 10 nM staurosporine for 24 h, *cyp1b1* −/− PC exhibited a twofold decrease in staurosporine-induced apoptosis compared with wild-type cells (Figure 3c).

To gain further insight into the role Cyp1B1 has in apoptosis, we examined the expression of pro- and anti-apoptotic members of the bcl-2 family. The bcl-2-associated-x protein (Bax) and Bim promote apoptosis by competing directly with bcl-2, an anti-apoptotic family member. Bax and Bim expression were lower in *cyp1b1* −/− PC compared with wild-type cells (Figure 3d–f). However, no significant change was observed in bcl-2 expression levels. The gene expression results were confirmed by western blotting for Bax (Figure 3d and e). Unfortunately, high-quality antibodies for detection of mouse bcl-2 and Bim are not commercially available. Thus, *cyp1b1* −/− PC expressed lower levels of Bax and Bim, and exhibited lower rates of apoptosis.

Increased Cellular Oxidative Stress in *cyp1b1* −/− PC

Many vascular pathologies and dysfunctions are presented with alterations in the cellular oxidative state. Oxidative and/or reductive reactions catalyzed by Cyp1B1 may have a significant role in the modulation of the vascular reductive state. We addressed whether exposure of *cyp1b1* +/+ and *cyp1b1* −/− PC to oxidative stress differentially impacted their viability. *Cyp1b1* +/+ and *cyp1b1* −/− PC were challenged with 150 μM H_2O_2 for 48 h. Figure 4a shows that *cyp1b1* −/− PC exhibited a twofold decrease in cell viability upon challenge with H_2O_2.

We next determined the level of ROS in *cyp1b1* +/+ and *cyp1b1* −/− PC using DHE staining. In Figure 4b, *cyp1b1* −/− PC exhibited increased fluorescence compared with *cyp1b1* +/+ PC, indicating higher levels of ROS in these cells. Furthermore, *Cyp1b1* +/+ cells incubated with Cyp1B1 inhibitor, TMS, displayed increased fluorescence, similar to *cyp1b1* −/− PC. Incubation with antioxidant NAC in the *cyp1b1* −/− PC revealed decreased fluorescence, indicating reduced levels of ROS. Both cell types exhibited increased fluorescence after exposure to H_2O_2; however, *cyp1b1* −/− PC exhibited a twofold increase in ROS levels after H_2O_2 compared to wild-type cells exposed to H_2O_2 (Figure 4c). Thus, expression and/or activity of Cyp1B1 play a significant role in maintaining the PC reductive state.

Cyp1b1 −/− PC are More Migratory and More Adhesive

The ability of PC to migrate and embed into the vascular basement membrane of the endothelium is essential for the maturation and stabilization of newly forming vessels.[35] We next examined the migratory characteristics of *cyp1b1* +/+ and *cyp1b1* −/− PC using a scratch wound assay. We observed accelerated wound closure in the *cyp1b1* −/− PC compared with *cyp1b1* +/+ PC after 72 h (Figure 5a and b). Similar results were observed using a transwell migration

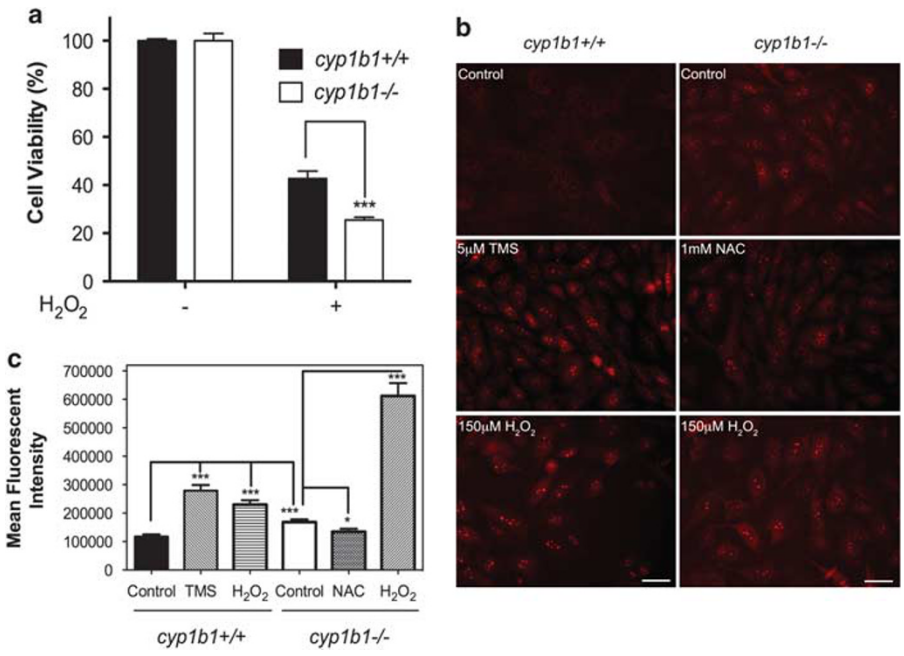

Figure 4 *Cyp1b1 −/−* retinal pericytes (PC) display higher oxidative stress. (**a**) Hydrogen peroxide (H_2O_2) toxicity of retinal PC was measured using the MTS assay. *Cyp1b1 +/+* and *cyp1b1 −/−* PC were incubated with 150 μM H_2O_2 for 48 h and demonstrated a 1.7-fold decrease in cell viability (***$P<0.0001$). (**b**) Oxidative stress was measured by dihydroethidium staining in the presence of solvent control DMSO; Cyp1B1 inhibitor, TMS; antioxidant, NAC; and H_2O_2 for 48 h. Scale bar, 20 μm. (**c**) Quantitative assessment of mean fluorescent intensity is shown (*$P<0.05$; ***$P<0.0001$).

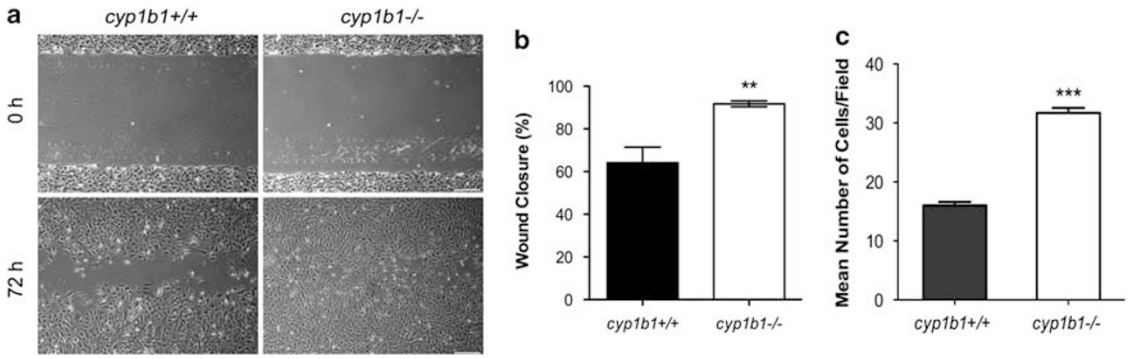

Figure 5 *Cyp1b1 −/−* retinal pericytes (PC) are more migratory. (**a**) Cell migration was determined by scratch wounding cell monolayers on uncoated tissue culture plates. Wound closure was monitored by photography. Scale bar indicates 100 μm. (**b**) Quantitative assessment of the data demonstrates an increase in wound closure in the *cyp1b1 −/−* PC (**$P<0.001$). (**c**) Transwell migration assays were performed to confirm the migration results. *Cyp1b1 −/−* PC demonstrated a twofold increase in migration (***$P<0.0001$).

assay. *Cyp1b1 −/−* PC demonstrated a twofold increase in the number of cells, which migrated through the membrane compared to *cyp1b1 +/+* cells (Figure 5c).

Alterations in the migratory properties of *cyp1b1 −/−* PC suggested that changes in their adhesive properties may occur. We next examined the cells' ability to adhere to various ECM proteins, including fibronectin, collagen I, laminin, and vitronectin (Figure 6). We observed a significant increase in the adhesion of *cyp1b1 −/−* PC to fibronectin, collagen I, and vitronectin compared with *cyp1b1 +/+* PC. Minimal adhesion to laminin was observed for both cell types.

Cell adhesion and migration requires binding to the ECM proteins through specific cell surface integrins. To determine whether the alterations observed in adhesion and migration of *cyp1b1 −/−* PC were in part due to altered integrin expression, we analyzed the expression of various integrins on the surface of *cyp1b1 +/+* and *cyp1b1 −/−* PC (Figure 7). *Cyp1b1 +/+* and *cyp1b1 −/−* PC expressed similar levels of $\alpha2$, $\alpha3$, $\alpha4$, αV, $\beta1$, $\beta8$, $\alpha5\beta1$, and $\alpha V\beta3$. Representative mean fluorescent intensities are shown in Figure 7a. However, *cyp1b1 −/−* PC expressed decreased levels of $\alpha5$ and $\alpha7$ integrins. The quantitative assessment of

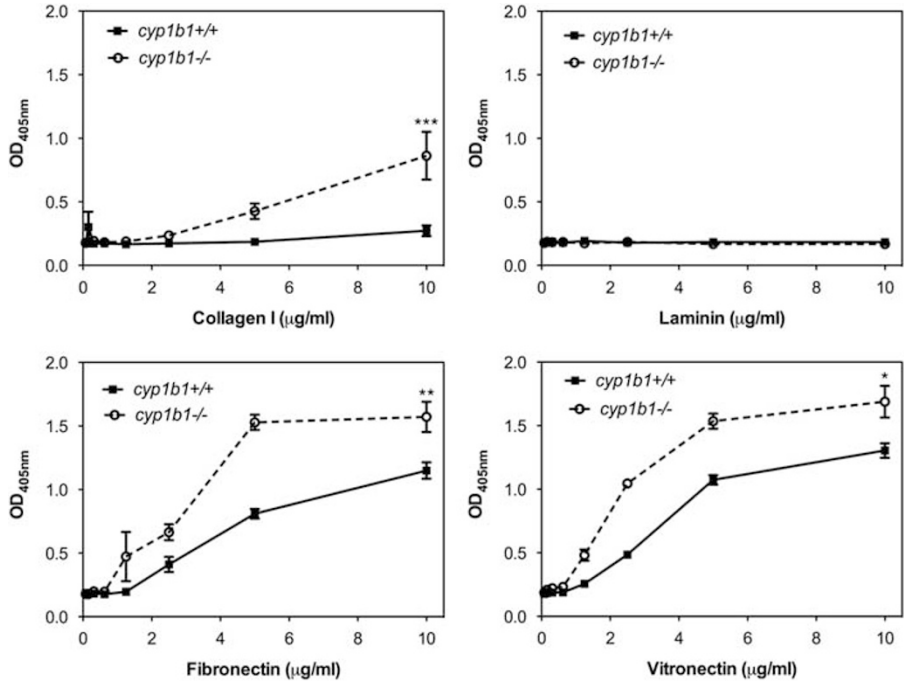

Figure 6 *Cyp1b1 −/−* retinal (PC) are more adherent. Adhesion of *cyp1b1 +/+* and *cyp1b1 −/−* PC to vitronectin, laminin, fibronectin and collagen I was determined as described in Experimental Procedures. Please note an increase in adhesion of cyp1b1 −/− PC to collagen I (***$P<0.0001$), fibronectin (**$P=0.0021$), and vitreonectin (*$P=0.021$).

results is shown in Figure 7b. A 50% decrease in α5 and a 70% decrease in α7 integrin levels were observed.

Alterations in Production of ECM Proteins in *cyp1b1 −/−* PC

The extracellular matrix serves many functions, including providing support, regulating the dynamic behavior of a cell, and acting as a depot for various cellular growth and soluble factors. Fibronectin, osteopontin, tenascin-C and thrombospondins are constituents of the ECM with significant roles in tissue remodeling and repair, cell migration and vascular inflammation. We examined the production of various ECM proteins in *cyp1b1 +/+* and *cyp1b1 −/−* PC by western blot analysis of conditioned medium and cell lysates (Figure 8a). Figure 8b shows the quantitative evaluation of the data. A three- and four-fold increase in the amount of TSP2 was detected in both lysate and conditioned medium of *cyp1b1 −/−* PC compared with *cyp1b1 +/+* PC, respectively. We observed a 60% reduction in the secretion of TSP1 and an 80% decrease in the secretion of tenascin-C in the conditioned medium of *cyp1b1 −/−* PC compared with *cyp1b1 +/+* cells. Osteopontin expression in both cell lysate and conditioned medium was undetectable in *cyp1b1 −/−* PC compared with wild-type cells.

Alterations in Intracellular Signaling Pathways of *cyp1b1 −/−* PC

The mitogen activated protein kinases (MAPK), including ERK1/2, regulate a diverse range of processes including cell proliferation, adhesion, and apoptosis. The Jun N-terminal Kinase (JNK) family has crucial roles in regulating cell stress, inflammation and apoptosis. Similar to JNK, the p38 MAPK cascade also responds to cell stress and inflammatory cytokines. Akt, a serine/threonine-specific kinase, is a regulator of multiple downstream processes, including glucose metabolism, apoptosis, cell proliferation, and migration. We assessed whether there were perturbations in any of these signaling pathways in *cyp1b1 −/−* PC. Both cell types exhibited similar phosphorylation and total p38, JNK, and Erk1/2 (Figure 9a). We observed an increase in phospho-Akt in *cyp1b1 −/−* PC compared with *cyp1b1 +/+* PC (Figure 9b). This is consistent with their reduced rate of apoptosis.

NF-κB proteins comprise a family of transcription factors that are involved in the control of a large number of cellular processes such as immune and inflammatory responses, cellular growth and apoptosis.[36,37] These transcription factors are persistently active in a number of disease states, including cancer, chronic inflammation, glaucoma, retinal diseases, and diabetes.[38–40] Increased oxidative stress can activate NF-κB signaling in cells.[41–43] To delineate whether a Cyp1B1 deficiency functionally impacts NF-κB signaling, we measured the level of phosphorylated and total p65 NF-κB. We observed a 1.5-fold increase in phospho-p65 and a 2.5-fold increase in total p65 expression in *cyp1b1 −/−* PC (Figure 9c and d). We analyzed several NF-κB target genes to confirm constitutive activation of the NF-κB pathway in the *cyp1b1 −/−* PC. We confirmed a 3.5-fold and a 2.5-fold

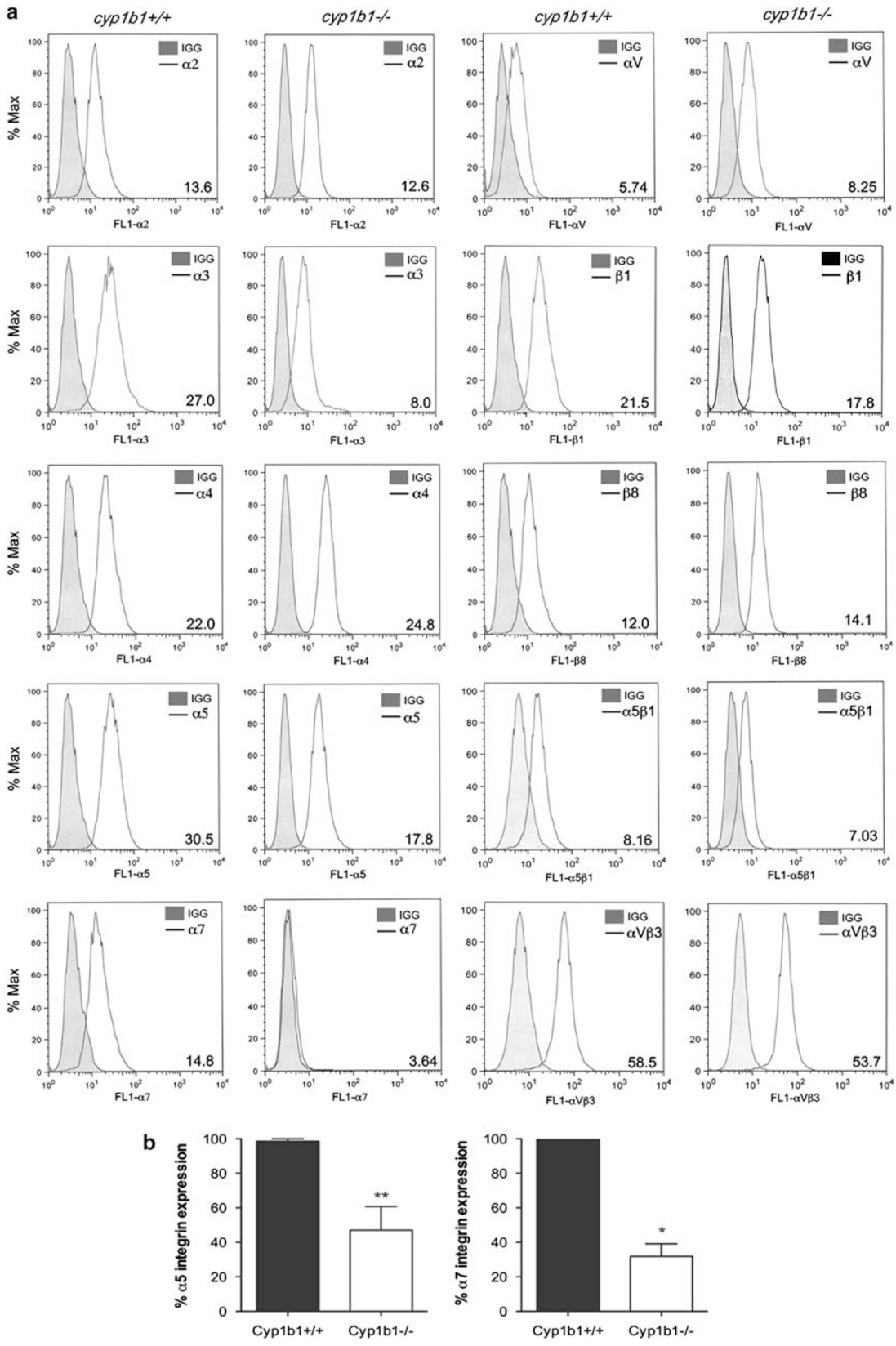

Figure 7 *Cyp1b1 −/−* retinal pericytes (PC) exhibit altered expression of integrins. (**a**) Expression of α1, α2, α3, α4, α5, α7, αV, β1, β8, α5β1, and αVβ3 integrins in *cyp1b1 +/+* and *cyp1b1 −/−* PC was determined by flow cytometry using specific antibodies as described in Materials and Methods. The shaded traces show staining in the absence of primary antibody. Representative mean fluorescent intensities are indicated in the bottom right corner of each panel. (**b**) Percent expression of α5 and α7 integrins was determined ($N=3$, $^{*}P<0.05$, $^{**}P<0.01$).

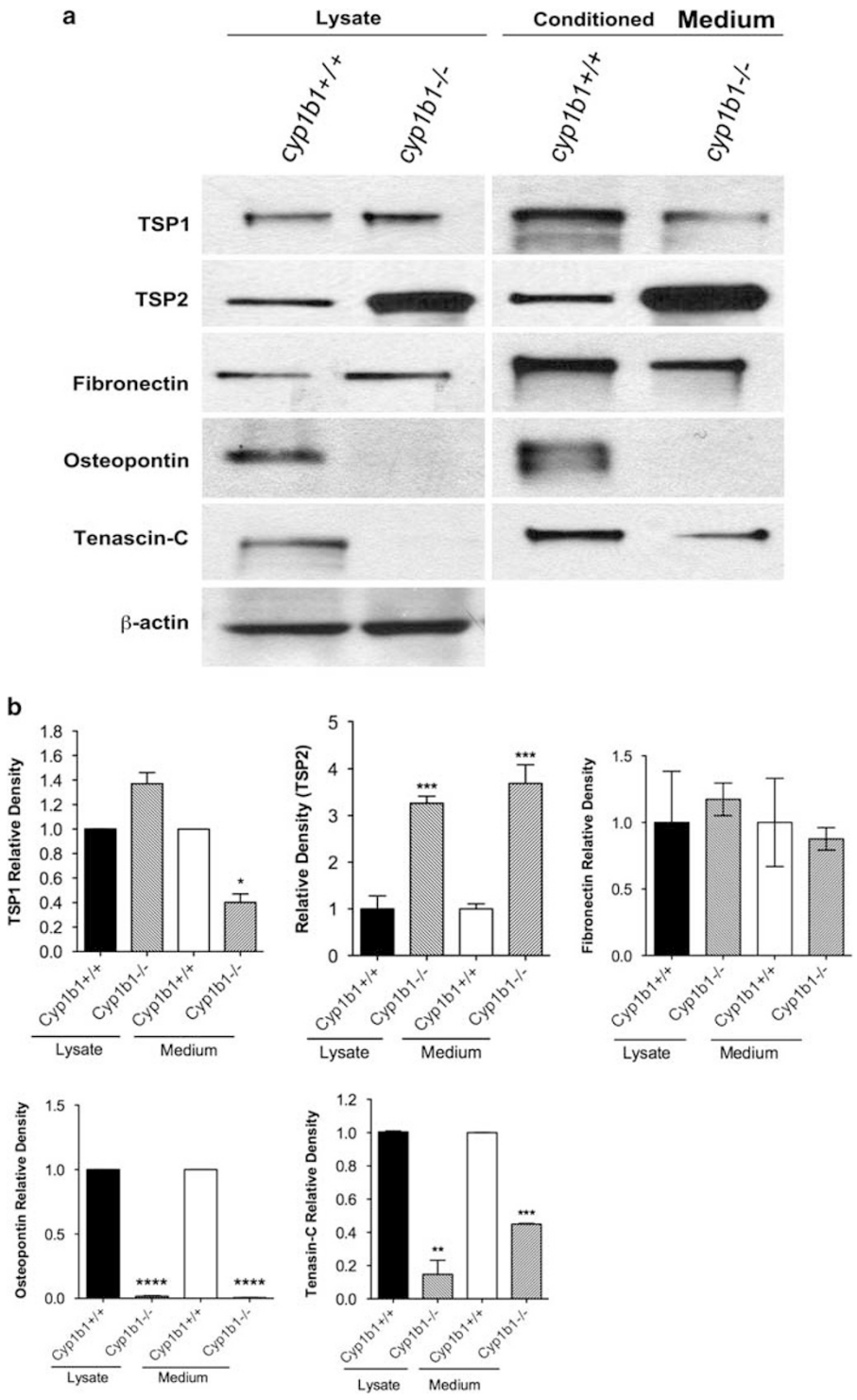

Figure 8 Altered expression of ECM proteins in *cyp1b1* $-/-$ retinal pericytes (PC). (**a**) *Cyp1b1* $+/+$ and *cyp1b1* $-/-$ PC were incubated for 2 days with serum-free PC medium. Cell lysates and conditioned medium were analyzed by western blot analysis for TSP1, TSP2, fibronectin, osteopontin, and tenascin-C using specific antibodies as described in Materials and Methods. (**b**) Quantitative assessment of band intensity was determined ($N=3$, $^{*}P<0.05$, $^{**}P<0.001$, $^{***}P<0.0001$, $^{****}P<0.00001$).

increase in NF-κB target gene mRNA for monocyte chemoattractant protein-1 (MCP-1) and tumor necrosis factor-alpha (TNF-α), two major inflammatory mediators produced by PC, respectively.[44]

Loss of Cyp1B1 Alters Capillary Morphogenesis and VEGF Secretion in PC

Stabilization of patent vessels is a critical function of PC.[29,35] We next investigated the impact a lack of Cyp1B1 has on the

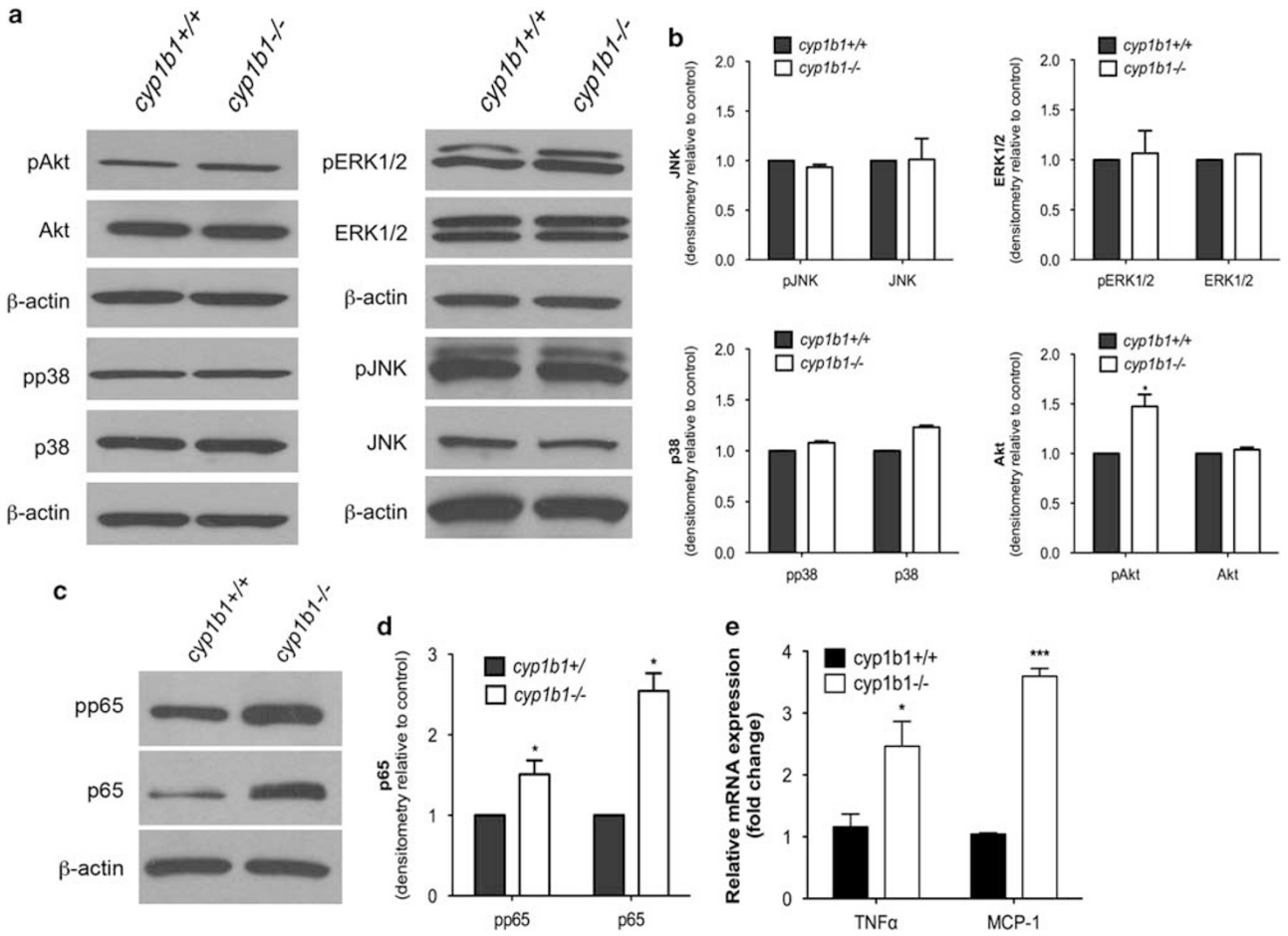

Figure 9 Alterations in cellular signaling pathways in *cyp1b1* −/− retinal pericytes (PC). (**a**) *Cyp1b1* +/+ and *cyp1b1* −/− PC were analyzed by western blot analysis for expression of phospho-Akt, total Akt, phospho-p38, total p38, phospho-Erk1/2, total Erk1/2, phospho-JNK, total JNK, and β-actin. (**b**) Quantification of band intensity demonstrated a 1.5-fold increase in phospho-Akt ($N=3$, $^*P<0.05$). (**c**) Levels of phospho-p65 NF-κB, total p65, and β-actin were determined by western blotting. (**d**) Quantitative assessment of the data ($N=3$, $^*P<0.05$). (**d**,**e**) Levels of RNA were assessed for NF-κB target genes MCP-1 ($^{***}P\leq0.0001$) and TNFα ($^*P<0.05$).

ability of retinal EC to undergo capillary morphogenesis. We have previously shown that a loss of Cyp1B1 in retinal EC attenuates capillary morphogenesis.[14,27] In Figure 10 a–h, we show that a lack of Cyp1B1 affects the co-culture of retinal EC and PC. Panels c and d show that PC do not form a tube-like network when plated alone in Matrigel. Together, retinal EC and PC (e) form a substantially improved tubular network compared with wild-type EC alone (a, $^*P<0.05$, comparison not indicated on graph). Co-culture of wild-type retinal EC with *cyp1b1* −/− PC showed a 50% decrease in tube formation (g) compared with control (e). In contrast, *cyp1b1* −/− retinal EC cultured with wild-type PC (h) displayed improved tube formation over the co-culture of *cyp1b1* −/− retinal EC and *cyp1b1* −/− PC (f). Through cell-to-cell contact and/or the secretion of multiple factors, the expression of Cyp1B1 is essential for capillary morphogenesis *in vitro*. The quantitative assessment of the mean number of branch points per field is shown in Figure 10i.

VEGF is a well-recognized inducer of angiogenesis. PC in the vasculature secrete VEGF to promote the survival of the endothelium.[45] We assessed whether secretion of VEGF into the medium was altered in the absence of Cyp1B1. A 2.2-fold decrease in VEGF levels was observed in *cyp1b1* −/− PC compared with *cyp1b1* +/+ PC (Figure 10j).

Mechanistically, signal transducers and activators of transcription (STAT), mainly STAT3, have an important role during angiogenesis, in both physiological and pathological conditions affecting cell survival, proliferation, inflammation, and oncogenesis. STAT3 participates in angiogenesis, in part, through the modulation of VEGF expression. We determined whether lack of Cyp1B1 impacted STAT3 phosphorylation (Figure 10k). We observed a fourfold decrease in the level of phosphorylated STAT3 in *cyp1b1* −/− PC compared with wild-type PC (Figure 10l). Thus, decreased signaling through the STAT3 pathway may be responsible for attenuation of VEGF expression in *cyp1b1* −/− PC.

DISCUSSION

PC are essential components of blood vessels, and are necessary for proper development, homeostasis, and organ

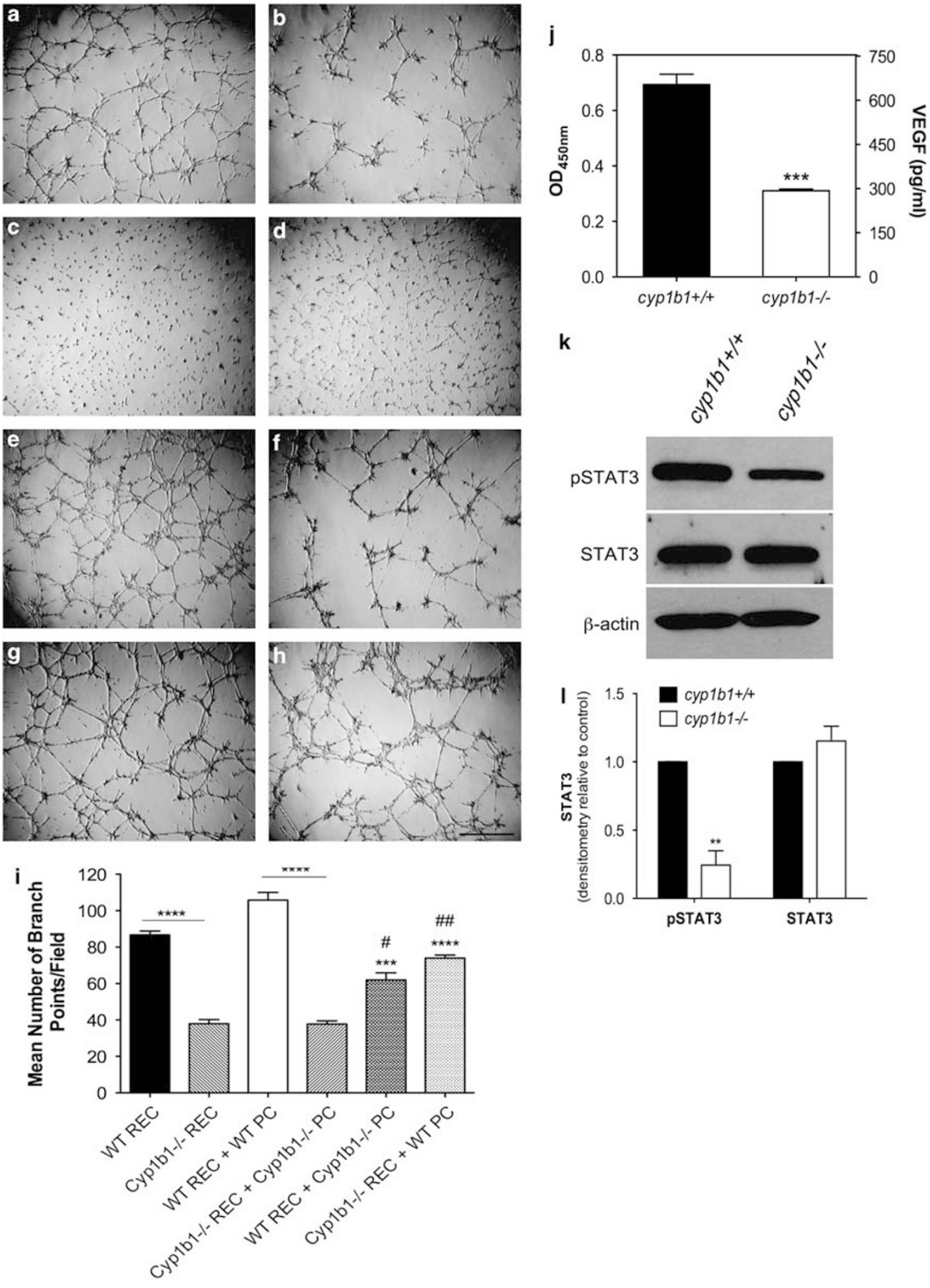

Figure 10 Loss of Cyp1B1 alters capillary morphogenesis and the production of vascular endothelial growth factor (VEGF) through the STAT3 pathway. (**a**–**h**) Capillary morphogenesis of retinal endothelial cell (EC) and pericytes (PC) was assessed by co-culturing cells in Matrigel for 18 h. Representative images are shown; (**a**) wild-type retinal EC, (**b**) *cyp1b1* −/− PC, (**c**) wild-type PC, (**d**) *cyp1b1* −/− PC, (**e**) wild-type retinal EC + PC, (**f**) *Cyp1b1* −/− retinal EC + *cyp1b1* −/− PC, (**g**) wild-type retinal EC + *cyp1b1* −/− PC, (**h**) *Cyp1b1* −/− retinal EC + wild-type PC. Scale bar represents 500 μm. (**i**) Mean number of branch points were counted ($N = 3$, $^{***}P < 0.0001$, $^{****}P < 0.00001$). (**j**) Analysis of VEGF levels in *cyp1b1* +/+ and *cyp1b1* −/− PC demonstrated a twofold decrease ($^{***}P \leq 0.0001$). (**k**) Levels of phospho-STAT3, total STAT3, and β-actin were determined by Western blotting. (**l**) Quantification of band intensity demonstrated a fourfold decrease in pSTAT3 ($N = 3$, $^{**}P < 0.001$).

function.[28,29] Alterations in PC recruitment, density, and attachment to the endothelium are associated with many vasculopathies, including diabetic retinopathy and hereditary stroke.[4] We recently showed that Cyp1B1 is constitutively expressed in EC from vascular beds of various tissues including retina, and has an important role in the regulation of the angiogenic properties of EC in culture and neovascularization *in vivo*.[14,27] Here we demonstrated that Cyp1B1 is constitutively expressed in retinal, heart and kidney PC and is further induced by TCDD, a known inducer of Cyp1B1 (Figure 1b and c). We showed that lack of Cyp1B1 was associated with enhanced proliferation and reduced apoptosis of PC. In addition, Cyb1b1 $-/-$ PC exhibited increased oxidative stress and sustained activation of NF-κB p65. These cells also exhibited significant defects in their adhesion and migration, concomitant with alterations in expression of various ECM proteins and their receptors. Together, our results suggest that Cyp1B1 expression and/or activity is essential for maintaining the cellular reductive state with significant impact on PC function.

Consistent and unequivocal identification of PC is challenging due to the heterogeneity of the PC population from different vascular bed sources and the isolation at different developmental stages. The multiple markers applied in Figures 1 and 2 to identify PC are neither specific nor stable in their expression, however, we observed expression of classical PC markers PDGFR-β, NG2, and αSMA. The heterogeneity in retinal PC was confirmed by expression of NG2 and αSMA in Figure 1e. Immunofluorescent staining revealed uniform, but relatively low expression of PDGFR-β (not shown), which may partially be due to low binding affinity of the antibody in this method or due to the limitation that not all PC express high levels of PDGFR-β.[46]

We also demonstrated that a loss of Cyp1B1 in PC resulted in increased proliferation concomitant with a decreased rate of apoptosis, both under basal and challenged conditions. The reduced rate of apoptosis may be attributed, at least in part, to the decreased expression of Bax and Bim, pro-apoptotic members of the Bcl-2 family, observed in the Cyp1B1-deficient cells. However, it is also possible that the increased phosphorylation of serine/threonine-specific Akt1 may contribute to the overall survival of PC in the Cyp1B1-deficient cells.

Oxidative stress occurs as a consequence of inequity between pro-and antioxidant systems, causing injury to biomolecules, such as nucleic acids, proteins, structural carbohydrates, and lipids. Polyunsaturated fatty acids are especially susceptible to peroxidation to form lipid peroxyl radicals. Peroxidation of lipids disturbs the assembly of membranes, leading to changes in permeability, alterations in ion transport and injury to mitochondria, which further potentiates ROS generation. We previously showed increases in 4-hydroxynonenal staining in retinas of *cyp1b1* $-/-$ mice compared with wild-type mice.[14] Here we showed that *cyp1b1* $-/-$ PC produce markedly more ROS than *cyp1b1* $+/+$ PC, similar to our previously reported results in EC.[14] Inhibition of Cyp1B1 enzymatic activity by incubation of TMS with *cyp1b1* $+/+$ PC also resulted in higher levels of ROS compared with control cells. Furthermore, incubation of *cyp1b1* $-/-$ PC with antioxidant NAC, lowered ROS levels. Cyp1B1 may influence the oxidative metabolism of endogenous substrates and maintain the cellular reductive state. Furthermore, a lack of Cyp1B1 expression and/or activity leads to the accumulation of ROS and increased oxidative stress in PC. Although the exact identity of the reactive species remains elusive, we believe these are oxygenated products of polyunsaturated fatty acids, which are normally metabolized by Cyp1B1 relieving intracellular oxidative stress.

NF-κB is a redox-sensitive transcription factor[47] with a central role in inflammation and is activated by increased intracellular oxygenated products. We observed increases in total p65 protein expression concomitant with increased p65 phosphorylation in *cyp1b1* $-/-$ PC. To confirm activation of NF-κB signaling, we investigated mRNA expression of two target genes, MCP-1 and TNF-α. Expression of these genes was increased in Cyp1B1-null PC compared with control cells. Pharmacological inhibitors and dominant-negative inhibition of NF-κB signaling are currently being investigated in our laboratory to further delineate the contribution of constitutive NF-κB activation to the *Cyp1b1*-null phenotype, both *in vitro* and *in vivo*.

The production of PDGF-BB by EC is essential for the recruitment of PC to newly forming microvessels.[35] The expression of PDGFR-β on the surface of PC is required for paracrine signaling and immediate attraction to emerging angiogenic sprouts. We observed a significant increase in the basal migration of *cyp1b1* $-/-$ PC. These changes in migration may be ancillary to altered adhesion to ECM proteins, fibronectin and vitronectin in *cyp1b1* $-/-$ PC, and activation of downstream signaling pathways. The changes in adhesion may be attributed, in part, to the changes in integrin expression and/or activity in these cells. Although we observed similar levels of $\alpha5\beta1$ and $\alpha v\beta3$-integrin expression (major fibronectin and vitronectin receptors), $\alpha5$ and $\alpha7$-integrin expression was decreased. Integrin $\alpha7$ has an important role in vascular development and integrity, and its loss is responsible for alterations in vascular remodeling and increased proliferation of VSMC.[48,49] The reduced expression of $\alpha7$ integrin is consistent with increased proliferation of *cyp1b1* $-/-$ PC and may contribute in a complex manner to the overall increase in survival observed here. We also observed that loss of Cyp1B1 in PC resulted in a dramatic upregulation of both cell associated and secreted TSP2. We previously showed that the loss of Cyp1B1 in EC results in increased expression of TSP2, a matricellular protein with anti-angiogenic activity.[14] In comparison, however, expression of TSP2 in retinal EC is significantly lower than that expressed in PC. The role TSP2 has in PC function is currently unknown. Together, our results suggest that Cyp1B1 expression is critical to the physiological

functions of PC including adhesion, proliferation, migration, and recruitment to newly forming microvessels.

Interactions between EC and PC are important in blood vessel maturation and stabilization.[29] Changes in cell–cell interactions are mediated through $\alpha 4\beta 1$-integrin on proliferating EC and VCAM-1 in proliferating PC.[50] The antagonism of these interactions prevents the adhesion of PC to the endothelium, resulting in EC dysfunction and dysregulation of angiogenesis. We observed a significant decrease in the expression of VCAM-1 in *cyp1b1* $-/-$ PC. A lack of Cyp1B1 may significantly hamper EC and PC interactions, and impede angiogenesis.[14] We observed disruptions in capillary morphogenesis using co-culture methods. Loss of Cyp1B1 in PC resulted in attenuation of EC capillary morphogenesis. In contrast, wild-type PC restored capillary morphogenesis of *cyp1b1* $-/-$ retinal EC. This suggests that through cell–cell interaction and/or the secretion of soluble mediators, Cyp1B1 is essential for the development, maturation, and stabilization of the vasculature. PC influence vessel stability by ECM deposition, production, and release of soluble factors that promote endothelial quiescence. Alterations in the production of the ECM may modulate EC and PC proliferation and migration and lead to defects in vascular stability. We observed a decrease in secreted TSP1 and tenascin-C from *cyp1b1* $-/-$ PC. Expression of cell associated and secreted osteopontin was also undetectable compared with wild-type cells. Osteopontin is involved in inflammatory cell migration, differentiation of osteoclasts and inflammatory cytokine production.[51–54] Knockdown of osteopontin leads to the amelioration of autoimmune arthritis and tumor metastasis. Phosphorylation of osteopontin is required for its ability to inhibit VSMC calcification.[55] A binding site exists in osteopontin for $\alpha 4\beta 1$-integrin. Alteration in ECM production in *cyp1b1* $-/-$ PC, along with aberrant VCAM-1 expression, may lead to the observed aberrant EC and PC interactions *in vitro* and attenuation of angiogenesis *in vivo*.

Retinal vascularization is a highly orchestrated process that is coordinated through complex interactions among EC, PC, and astrocytes, and is tightly regulated by a balanced production of pro- and anti-angiogenic factors.[56,57] VEGF is one of the most important mediators of ocular angiogenesis. Production of VEGF by PC is important for survival of EC and vascular integrity.[45] *Cyp1b1* $-/-$ PC exhibited a two-fold decrease in VEGF production. Decreased VEGF production was consistent with enhanced migration and proliferation of PC. Greenberg *et al*[58] recently showed that VEGF may act as a negative regulator of PC function and vessel maturation. Increasing studies show that STAT3 participates in regulating angiogenesis, largely in part, through modulation of VEGF expression.[59] STAT3 is a direct transcriptional activator of the *VEGF* gene by binding to the VEGF promoter.[60] Activated STAT3 upregulates VEGF expression, and promotes tumor angiogenesis.[60] We observed a significant decrease in the level of STAT3 serine 727 phosphorylation in *cyp1b1* $-/-$ PC. Decreased production of VEGF by *cyp1b1* $-/-$ PC may contribute to the EC dysfunction and attenuation of neovascularization we previously reported in *cyp1b1* $-/-$ mice.

In summary, we demonstrated in retinal PC that expression and/or activity of Cyp1B1 is essential for the appropriate proliferation and migration of PC and subsequent interactions with the underlying endothelium. Cyp1B1 deficiency in PC resulted in increased oxidative stress, sustained activation of NF-κB, increased expression of TSP2, and decreased expression of VEGF. Together, our results indicate that the expression of Cyp1B1 is essential for maintaining the cellular reductive state and normal PC function.

ACKNOWLEDGEMENTS

We thank Dr Zafer Gurel and SunYoung Park for their assistance in conducting experiments. This work supported in part by NIH grants T32 ES007015, EY016995, EY018179, RC4 EY021357, P30 CA014520 University of Wisconsin Paul P. Carbone Cancer Center Support grant, P30 EY016665, and an unrestricted departmental award from Research to Prevent Blindness. NS is a recipient of a Research Award from American Diabetes Association (1-20-BS-160) and Retina Research Foundation. TLP is recipient of a Kirschstein-NRSA Fellowship Award (F31 EY021091) and a Science and Medicine Graduate Research Scholar at the University of Wisconsin-Madison.

DISCLOSURE/CONFLICT OF INTEREST

The authors declare no conflict of interest.

1. Hellstrom M, Kalen M, Lindahl P, *et al.* Role of PDGF-B and PDGFR-beta in recruitment of vascular smooth muscle cells and pericytes during embryonic blood vessel formation in the mouse. Development 1999;126:3047–3055.
2. Rolny C, Nilsson I, Magnusson P, *et al.* Platelet-derived growth factor receptor-beta promotes early endothelial cell differentiation. Blood 2006;108:1877–1886.
3. von Tell D, Armulik A, Betsholtz C. Pericytes and vascular stability. Exp Cell Res 2006;312:623–629.
4. Hayden MR, Yang Y, Habibi J, *et al.* Pericytopathy: Oxidative stress and impaired cellular longevity in the pancreas and skeletal muscle in metabolic syndrome and type 2 diabetes. Oxid Med Cell Longev 2010;3:290–303.
5. Fleming I. Vascular cytochrome p450 enzymes: physiology and pathophysiology. Trends Cardiovasc Med 2008;18:20–25.
6. Coon MJ. Cytochrome P450: nature's most versatile biological catalyst. Annu Rev Pharmacol Toxicol 2005;45:1–25.
7. Stoilov I, Rezaie T, Jansson I, *et al.* Expression of cytochrome P4501b1 (Cyp1b1) during early murine development. Mol Vis 2004;10:629–636.
8. Murray GI, Melvin WT, Greenlee WF, *et al.* Regulation, function, and tissue-specific expression of cytochrome P450 CYP1B1. Annu Rev Pharmacol Toxicol 2001;41:297–316.
9. Hakkola J, Pasanen M, Pelkonen O, *et al.* Expression of CYP1B1 in human adult and fetal tissues and differential inducibility of CYP1B1 and CYP1A1 by Ah receptor ligands in human placenta and cultured cells. Carcinogenesis 1997;18:391–397.
10. Choudhary D, Jansson I, Rezaul K, *et al.* Cyp1b1 protein in the mouse eye during development: an immunohistochemical study. Drug Metab Dispos 2007;35:987–994.
11. Bejjani BA, Xu L, Armstrong D, *et al.* Expression patterns of cytochrome P4501B1 (Cyp1b1) in FVB/N mouse eyes. Exp Eye Res 2002;75:249–257.
12. Ikegwuonu FI, Christou M, Jefcoate CR. Regulation of cytochrome P4501B1 (CYP1B1) in mouse embryo fibroblast (C3H10T1/2) cells by protein kinase C (PKC). Biochem Pharmacol 1999;57:619–630.
13. Zhang L, Savas U, Alexander DL, *et al.* Characterization of the mouse Cyp1B1 gene. Identification of an enhancer region that directs aryl hydrocarbon receptor-mediated constitutive and induced expression. J Biol Chem 1998;273:5174–5183.
14. Tang Y, Scheef EA, Wang S, *et al.* CYP1B1 expression promotes the proangiogenic phenotype of endothelium through decreased

intracellular oxidative stress and thrombospondin-2 expression. Blood 2009;113:744–754.
15. Sutter TR, Tang YM, Hayes CL, *et al.* Complete cDNA sequence of a human dioxin-inducible mRNA identifies a new gene subfamily of cytochrome P450 that maps to chromosome 2. J Biol Chem 1994;269:13092–13099.
16. Kerzee JK, Ramos KS. Constitutive and inducible expression of Cyp1a1 and Cyp1b1 in vascular smooth muscle cells: role of the Ahr bHLH/PAS transcription factor. Circ Res 2001;89:573–582.
17. Heidel SM, Czuprynski CJ, Jefcoate CR. Bone marrow stromal cells constitutively express high levels of cytochrome P4501B1 that metabolize 7,12-Dimethylbenz[a]anthracene. Mol Pharmacol 1998;54:1000–1006.
18. Eltom SE, Zhang L, Jefcoate CR. Regulation of cytochrome P-450 (CYP) 1B1 in mouse Hepa-1 variant cell lines: a possible role for aryl hydrocarbon receptor nuclear translocator (ARNT) as a suppressor of CYP1B1 gene expression. Mol Pharmacol 1999;55:594–604.
19. Eltom SE, Larsen MC, Jefcoate CR. Expression of CYP1B1 but not CYP1A1 by primary cultured human mammary stromal fibroblasts constitutively and in response to dioxin exposure: role of the Ah receptor. Carcinogenesis 1998;19:1437–1444.
20. Conway DE, Sakurai Y, Weiss D, *et al.* Expression of CYP1A1 and CYP1B1 in human endothelial cells: regulation by fluid shear stress. Cardiovasc Res 2009;81:669–677.
21. Brake PB, Arai M, As-Sanie S, *et al.* Developmental expression and regulation of adrenocortical cytochrome P4501B1 in the rat. Endocrinology 1999;140:1672–1680.
22. Buters JT, Sakai S, Richter T, *et al.* Cytochrome P450 CYP1B1 determines susceptibility to 7,12-dimethylbenz[a]anthracene-induced lymphomas. Proc Natl Acad Sci USA 1999;96:1977–1982.
23. Choudhary D, Jansson I, Stoilov I, *et al.* Metabolism of retinoids and arachidonic acid by human and mouse cytochrome P450 1b1. Drug Metab Dispos 2004;32:840–847.
24. Stoilov I, Akarsu AN, Sarfarazi M. Identification of three different truncating mutations in cytochrome P4501B1 (CYP1B1) as the principal cause of primary congenital glaucoma (Buphthalmos) in families linked to the GLC3A locus on chromosome 2p21. Hum Mol Genet 1997;6:641–647.
25. Bejjani BA, Lewis RA, Tomey KF, *et al.* Mutations in CYP1B1, the gene for cytochrome P4501B1, are the predominant cause of primary congenital glaucoma in Saudi Arabia. Am J Hum Genet 1998;62:325–333.
26. Libby RT, Smith RS, Savinova OV, *et al.* Modification of ocular defects in mouse developmental glaucoma models by tyrosinase. Science 2003;299:1578–1581.
27. Tang Y, Scheef EA, Gurel Z, *et al.* CYP1B1 and endothelial nitric oxide synthase combine to sustain proangiogenic functions of endothelial cells under hyperoxic stress. Am J Physiol Cell Physiol 2010;298:C665–C678.
28. Hirase T, Node K. Endothelial dysfunction as a cellular mechanism for vascular failure. Am J Physiology—Heart Circulatory Physiol 2012;302:H499–H505.
29. Armulik A, Genove G, Betsholtz C. Pericytes: developmental, physiological, and pathological perspectives, problems, and promises. Dev Cell 2011;21:193–215.
30. DiMaio TA, Sheibani N. PECAM-1 isoform-specific functions in PECAM-1-deficient brain microvascular endothelial cells. Microvasc Res 2008;75:188–201.
31. Zhao W, Parrish AR, Ramos KS. Constitutive and inducible expression of cytochrome P450IA1 and P450IB1 in human vascular endothelial and smooth muscle cells. In Vitro Cell Dev Biol Anim 1998;34:671–673.
32. Gibson P, Gill JH, Khan PA, *et al.* Cytochrome P450 1B1 (CYP1B1) is overexpressed in human colon adenocarcinomas relative to normal colon: implications for drug development. Mol Cancer Ther 2003;2:527–534.
33. Wang XQ, Lindberg FP, Frazier WA. Integrin-associated protein stimulates alpha2beta1-dependent chemotaxis via Gi-mediated inhibition of adenylate cyclase and extracellular-regulated kinases. J Cell Biol 1999;147:389–400.
34. Scheef EA, Sorenson CM, Sheibani N. Attenuation of proliferation and migration of retinal pericytes in the absence of thrombospondin-1. Am J Physiol Cell Physiol 2009;296:C724–C734.
35. Armulik A, Abramsson A, Betsholtz C. Endothelial/pericyte interactions. Circ Res 2005;97:512–523.
36. Perkins ND. Integrating cell-signalling pathways with NF-kappaB and IKK function. Nat Rev Mol Cell Biol 2007;8:49–62.
37. Tabruyn SP, Griffioen AW. NF-kappaB: a new player in angiostatic therapy. Angiogenesis 2008;11:101–106.
38. Partridge J, Carlsen H, Enesa K, *et al.* Laminar shear stress acts as a switch to regulate divergent functions of NF-kappaB in endothelial cells. FASEB J. 2007;21:3553–3561.
39. Romeo G, Liu WH, Asnaghi V, *et al.* Activation of nuclear factor-kappaB induced by diabetes and high glucose regulates a proapoptotic program in retinal pericytes. Diabetes 2002;51:2241–2248.
40. Xu C, Shen G, Chen C, *et al.* Suppression of NF-kappaB and NF-kappaB-regulated gene expression by sulforaphane and PEITC through IkappaBalpha, IKK pathway in human prostate cancer PC-3 cells. Oncogene 2005;24:4486–4495.
41. Bonello S, Zahringer C, BelAiba RS, *et al.* Reactive oxygen species activate the HIF-1alpha promoter via a functional NFkappaB site. Arterioscler Thromb Vasc Biol 2007;27:755–761.
42. Donato AJ, Eskurza I, Silver AE, *et al.* Direct evidence of endothelial oxidative stress with aging in humans: relation to impaired endothelium-dependent dilation and upregulation of nuclear factor-kappaB. Circ Res 2007;100:1659–1666.
43. Kowluru RA, Koppolu P, Chakrabarti S, *et al.* Diabetes-induced activation of nuclear transcriptional factor in the retina, and its inhibition by antioxidants. Free Radic Res 2003;37:1169–1180.
44. Nehmé A, Edelman J. Dexamethasone inhibits high glucose–, TNF-α–, and IL-1β–induced secretion of inflammatory and angiogenic mediators from retinal microvascular pericytes. Invest Ophthalmol Vis Sci 2008;49:2030–2038.
45. Darland DC, Massingham LJ, Smith SR, *et al.* Pericyte production of cell-associated VEGF is differentiation-dependent and is associated with endothelial survival. Dev Biol 2003;264:275–288.
46. Song S, Ewald AJ, Stallcup W, *et al.* PDGFRbeta+ perivascular progenitor cells in tumours regulate pericyte differentiation and vascular survival. Nat Cell Biol 2005;7:870–879.
47. Shono T, Ono M, Izumi H, *et al.* Involvement of the transcription factor NF-kappaB in tubular morphogenesis of human microvascular endothelial cells by oxidative stress. Mol Cell Biol 1996;16:4231–4239.
48. Flintoff-Dye NL, Welser J, Rooney J, *et al.* Role for the alpha7beta1 integrin in vascular development and integrity. Dev Dyn 2005;234:11–21.
49. Welser JV, Lange N, Singer CA, *et al.* Loss of the alpha7 integrin promotes extracellular signal-regulated kinase activation and altered vascular remodeling. Circ Res 2007;101:672–681.
50. Garmy-Susini B, Jin H, Zhu Y, *et al.* Integrin alpha4beta1-VCAM-1-mediated adhesion between endothelial and mural cells is required for blood vessel maturation. J Clin Invest 2005;115:1542–1551.
51. Dai J, Peng L, Fan K, *et al.* Osteopontin induces angiogenesis through activation of PI3K/AKT and ERK1/2 in endothelial cells. Oncogene 2009;28:3412–3422.
52. Lund SA, Giachelli CM, Scatena M. The role of osteopontin in inflammatory processes. J Cell Commun Signal 2009;3:311–322.
53. Speer MY, Chien YC, Quan M, *et al.* Smooth muscle cells deficient in osteopontin have enhanced susceptibility to calcification *in vitro*. Cardiovasc Res 2005;66:324–333.
54. Scatena M, Liaw L, Giachelli CM. Osteopontin: a multifunctional molecule regulating chronic inflammation and vascular disease. Arterioscler Thromb Vasc Biol 2007;27:2302–2309.
55. Jono S, Peinado C, Giachelli CM. Phosphorylation of osteopontin is required for inhibition of vascular smooth muscle cell calcification. J Biol Chem 2000;275:20197–20203.
56. Fruttiger M. Development of the retinal vasculature. Angiogenesis 2007;10:77–88.
57. Wang S, Wu Z, Sorenson CM, *et al.* Thrombospondin-1-deficient mice exhibit increased vascular density during retinal vascular development and are less sensitive to hyperoxia-mediated vessel obliteration. Dev Dyn 2003;228:630–642.
58. Greenberg JI, Shields DJ, Barillas SG, *et al.* A role for VEGF as a negative regulator of pericyte function and vessel maturation. Nature 2008;456:809–813.
59. Bartoli M, Platt D, Lemtalsi T, *et al.* VEGF differentially activates STAT3 in microvascular endothelial cells. FASEB J 2003;17:1562–1564.
60. Chen Z, Han ZC. STAT3: a critical transcription activator in angiogenesis. Med Res Rev 2008;28:185–200.